

AD-A163 252

ANALYSIS OF HELICAL WAVEGUIDE(U) NAVAL RESEARCH LAB  
WASHINGTON DC 5 AMN ET AL. 23 DEC 85 NRL-MR-5620

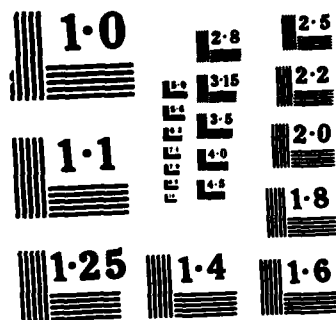
1/1

UNCLASSIFIED

F/G 9/1

NL

						END							
						FORMED							
						---							
						ETC							



NATIONAL BUREAU OF STANDARDS  
MICROCOPY RESOLUTION TEST CHART

AD-A163 252

2

NRL Memorandum Report 5620

## Analysis of Helical Waveguide

S. AHN AND A. K. GANGULY

*Electronics Technology Division*

December 23, 1985



NAVAL RESEARCH LABORATORY  
Washington, D.C.

Approved for public release; distribution unlimited.

DTIC  
ELECTE  
JAN 15 1986  
S A D

86 1 15 071

DTIC FILE COPY

AD-A163252

## REPORT DOCUMENTATION PAGE

1a. REPORT SECURITY CLASSIFICATION <b>UNCLASSIFIED</b>			1b. RESTRICTIVE MARKINGS		
2a. SECURITY CLASSIFICATION AUTHORITY			3. DISTRIBUTION/AVAILABILITY OF REPORT Approved for public release; distribution is unlimited.		
2b. DECLASSIFICATION/DOWNGRADING SCHEDULE					
4. PERFORMING ORGANIZATION REPORT NUMBER(S) NRL Memorandum Report 5620			5. MONITORING ORGANIZATION REPORT NUMBER(S)		
6a. NAME OF PERFORMING ORGANIZATION Naval Research Laboratory		6b. OFFICE SYMBOL (if applicable) 6840		7a. NAME OF MONITORING ORGANIZATION Naval Research Laboratory	
6c. ADDRESS (City, State, and ZIP Code) 4555 Overlook Avenue Washington, DC 20375-5000			7b. ADDRESS (City, State, and ZIP Code) 4555 Overlook Avenue Washington, DC 20375-5000		
8a. NAME OF FUNDING/SPONSORING ORGANIZATION Office of Naval Research		8b. OFFICE SYMBOL (if applicable)		9. PROCUREMENT INSTRUMENT IDENTIFICATION NUMBER	
8c. ADDRESS (City, State, and ZIP Code) Arlington, VA			10. SOURCE OF FUNDING NUMBERS		
			PROGRAM ELEMENT NO. 61153N		TASK NO. RR021-05-4B
			PROJECT NO.		WORK UNIT DN380-056
11. TITLE (Include Security Classification) Analysis of Helical Waveguide					
12. PERSONAL AUTHOR(S) Ahn, S. and Ganguly, A.K.					
13a. TYPE OF REPORT NRL Memo Report		13b. TIME COVERED FROM TO		14. DATE OF REPORT (Year, Month, Day) 1985 December 23	
				15. PAGE COUNT 34	
16. SUPPLEMENTARY NOTATION					
17. COSATI CODES			18. SUBJECT TERMS (Continue on reverse if necessary and identify by block number)		
FIELD	GROUP	SUB-GROUP	Traveling wave tube Efficiency		
			Helix structure Backward wave oscillation		
			Gain		
19. ABSTRACT (Continue on reverse if necessary and identify by block number) The dispersion characteristics of the large diameter helical waveguide are calculated using Pierce's small signal theory. The backward wave oscillation poses a serious problem for the development of this circuit as a broad-band, high gain amplifier. The gain of the backward waves is in general higher than the gain of the forward waves. For the first space harmonic ( $m = 1$ ) mode, the forward and the backward wave gains are, respectively, 2.17 dB/cm and 2.24 dB/cm. The bandwidth is 40% for a total gain of 30 dB if the backward waves are ignored. The onset of the backward wave oscillation limits the bandwidth to 5% for such high gain. The threshold interaction length for the onset of oscillation is also calculated. If the oscillations are not suppressed, the total gain of the circuit is limited to about 12 dB. At this low gain, the bandwidth can be as high as 57%. The device performs better with the low order space harmonic modes. Not only the gain and the bandwidth are larger for the low order modes but the ratio of the backward to forward wave gains and the number of the backward waves excited are also smaller.					
20. DISTRIBUTION/AVAILABILITY OF ABSTRACT <input type="checkbox"/> UNCLASSIFIED/UNLIMITED <input checked="" type="checkbox"/> SAME AS RPT. <input type="checkbox"/> DTIC USERS			21. ABSTRACT SECURITY CLASSIFICATION <b>UNCLASSIFIED</b>		
22a. NAME OF RESPONSIBLE INDIVIDUAL S. Ahn			22b. TELEPHONE (Include Area Code) (202) 767-3382		22c. OFFICE SYMBOL 6840

## CONTENTS

I.	INTRODUCTION .....	1
II.	DISPERSION CHARACTERISTICS OF THE EMPTY GUIDE .....	2
III.	WAVE IMPEDANCE OF THE HELICAL WAVEGUIDE .....	3
IV.	INTERACTION IMPEDANCE AND GAIN .....	4
V.	START OSCILLATION CURRENT .....	7
VI.	RESULTS AND DISCUSSIONS .....	9
VII.	CONCLUSION .....	13
VIII.	ACKNOWLEDGMENT .....	13
IX.	REFERENCES .....	13



Accession For	
NTIS CPA&I	<input checked="" type="checkbox"/>
DTIC TAB	<input type="checkbox"/>
Unannounced	<input type="checkbox"/>
Justification	
By	
Distribution	
Availability Codes	
Dist	Avail and/or Special
A-1	

# ANALYSIS OF HELICAL WAVEGUIDE

## I. INTRODUCTION

High power ( $\sim 10$  kW) and broadband ( $> 30\%$ ) millimeter wave amplifiers operating with low energy (10-15 keV) electron beam will be extremely useful in airborne Naval electronic warfare systems. The frequency range of interest is 60-100 GHz. In this frequency range, the conventional slow wave circuits such as klystrons and TWTs have low average power due to the small size of the circuit (the circuit diameter is about 0.2 wavelength). The power limit in the small diameter circuit is imposed by the low thermal dissipation capability and the limiting beam power density of a good quality beam that can be generated by an electron gun. The fast-wave amplifiers such as gyro-TWTs and gyroklystrons can produce high power in this frequency range but generally require relativistic electron beam and superconducting magnets. Consequently, new design concepts of slow wave circuits are being explored to increase their power handling capability. One such concept [1] was examined in 1957. The circuit was formed by spiralling a rectangular waveguide into a large diameter helix. An annular electron beam with large diameter can be injected axially through a slit gap in the wall and will experience a periodic field provided by the helical waveguide. The large size of the beam permits the injection of a high power beam while staying within the limiting beam power density mentioned earlier. However, as will be shown later, the interaction impedance and the gain of this circuit is small because of its large diameter.

The dispersion characteristics of the empty helical waveguide were obtained by Waldron [1]. The bandwidth of the circuit was estimated to be less than 5% due to the presence of the backward waves. It was concluded that the circuit was not of practical use as a broad-band amplifier and the interaction of the beam with this circuit was not investigated. In a series of experiments at the Naval Research Laboratory, Smith et al [2] are reexamining this circuit and assessing its feasibility as a broad-band, high power amplifier by suppressing the generation of the backward waves. To determine the role played by the backward waves in reducing the bandwidth and to devise means for their suppression, it is necessary to calculate the relative gain of the forward and the backward waves and the threshold for the onset of the backward wave oscillations. In this paper, we calculate these circuit characteristics by a small signal analysis of the dispersion relation of the helical waveguide in the presence of an electron beam. In Sec. II, we show the dispersion characteristics of the empty helical waveguide to give some

understanding of the mode structure of this device and the limitations in bandwidth due to the backward waves. The wave impedance of the circuit is calculated in Sec. III. Since the structure is periodic, the field is expressed as an infinite sum of space harmonics. Because of their lower phase velocity, the modes with high space harmonic number are particularly suitable for obtaining synchronism with low energy beams. The wave impedance, however, decreases rapidly for higher space harmonics. The interaction impedance, the gain and the bandwidth are calculated in Sec. IV using Pierce [3] method. This approximation is used partly due to the complexity of the circuit and partly due to the low voltage operation of the device. The backward wave gain ( $\sim 2.24$  dB/cm) is found higher than the forward wave gain ( $\sim 2.17$  dB/cm) but the bandwidth of the backward wave is extremely narrow. The threshold condition for the occurrence of the backward wave oscillation is calculated in Sec. V. It is found that the total gain in this circuit is limited to about 12 dB if the backward waves are not suppressed. The results for some specific design parameters are given in Sec. VI.

## II. DISPERSION CHARACTERISTICS OF THE EMPTY GUIDE

The helical waveguide with the slit gap for beam passage will be considered to find its wave dispersion. A schematic of the structure is shown in Fig. 1. The height and the width of the rectangular waveguide are denoted, respectively, by  $w$  and  $l$ . The pitch and the average radius (distance from the axis to the center of the rectangular guide) of the helical spiral will be denoted by  $L$  and  $R_0$ , respectively. The perturbations of the  $TE_{10}^0$  rf field in the transverse plane due to the slit gap and the spiralling of the waveguide will be neglected in the calculation of the dispersion relations. The dispersion relation for the  $TE_{10}^0$  mode of the straight rectangular waveguide is given by

$$c^2 \beta_z^2 = \omega^2 - \omega_c^2 \quad (1)$$

where  $\beta_z$  and  $\omega_c = \pi c/w$  are the axial wave number and the angular cut-off frequency of the straight waveguide, and  $\omega$  and  $c$  are, respectively, the wave angular frequency and the velocity of light in vacuum.  $\beta_z$  determines the phase shift along the helical direction of the spiraled waveguide. The fundamental axial wave number  $\beta_0$  of the spiraled waveguide is given by

$$\beta_0 = \beta_z L_0 / L \quad (2)$$

where  $L_0 = \{4\pi^2 R_0^2 + L^2\}^{1/2}$  is the length of the spiral in one pitch. Due to the presence of the periodicity, the phase constant of the  $m$ -th space harmonic may be written as

$$\beta_m = \beta_0 + 2\pi m / L \quad (m : \text{integer}) . \quad (3)$$

Therefore, the dispersion equation of the "empty" spiraled waveguide can be written as follows\*:

$$\beta_m = \frac{L_0}{cL} \sqrt{\omega^2 - \omega_c^2} + \frac{2\pi m}{L} = \beta_0 + 2\pi m/L \quad (4a)$$

and

$$\omega^2 = \omega_c^2 + c^2 (\beta_m L - 2\pi m)^2 / L_0^2 \quad (4b)$$

The phase velocity of the  $TE_{10}^*$  mode along the waveguide axis is clearly seen slowed down in Eq. (4), and thus we can find a set of circuit parameters which give rise to the synchronization condition for the circuit and beam interaction. As shown in Fig. 2, we can choose not only a high axial wave mode (e.g.,  $m = 4$ ) but also the fundamental wave ( $m = 0$ ) to meet this wide band synchronization.

The interaction of the forward wave ( $m = 0$ ) with backward wave ( $m = -n$ ) occurs at

$$\beta L = m\pi$$

and the corresponding frequency is

$$\omega_n = c \{ \pi^2 / w^2 + m^2 \pi^2 / [4\pi^2 R_0^2 + L^2] \}^{1/2}. \quad (5)$$

This equation yields a relative bandwidth as given below

$$\omega_n / \omega_{n-1} \approx (\pi^2 + n^2)^{1/2} / (\pi^2 + (n-1)^2)^{1/2}.$$

Thus

$$\omega_1 / \omega_c = 1.05, \omega_2 / \omega_1 = 1.13, \omega_3 / \omega_2 = 1.166, \omega_4 / \omega_3 = 1.171, \omega_5 / \omega_4 = 1.161.$$

### III. WAVE IMPEDANCE OF THE HELICAL WAVEGUIDE

Since the structure is periodic in the  $z$ -direction and has helical symmetry, it is possible to express the field acting on the electrons by an infinite sum of space harmonics

$$E(z, r, \phi) = \sum_n E_n \sin \frac{\pi}{w} (r - R_0) e^{-i\beta_0 z} e^{in\left(\phi - \frac{2\pi z}{L}\right)}. \quad (6)$$

\*The cutoff frequency will increase for this fundamental TE mode when we consider the effect of the slot for the beam passage. We ignore this effect in this paper.



In writing Eq. (6), it is assumed that the annular opening does not perturb the empty guide modes. By Fourier transform of Eq. (6), we obtain

$$E_m = \frac{1}{L} \int_0^L E(z, r, \phi) e^{i(\beta_0 + 2\pi m/L)z} dz$$

$$= -\frac{V}{Ll} \int_{-l/2}^{l/2} e^{i\beta_m z} dz = -\frac{lE_0}{L} \cdot \frac{\sin \xi}{\xi}, \quad (7)$$

where  $\xi = l\beta_m/2$  and  $E_0 = V/l$ . The circuit impedance  $K_m$  for the  $m$ -th mode may be written as

$$K_m = E_m^2 / (2\beta_m^2 W_T), \quad (8)$$

with  $E_m$  given in Eq. (7).  $W_T$  is the power flow in the  $z$ -direction and is the same as the power flow through the straight waveguide,

$$W_T = (\mu\omega\beta_g c^2 / 2\omega_c^2) \int H_z^2 dA \quad (A: \text{cross-sectional area}). \quad (9)$$

Since  $H_z = -(\omega_c^2 w E_0 / \pi c^2 \mu \omega) \cos(\pi x/w)$  for  $TE_{10}^0$  mode, we find

$$W_T = E_0^2 l w \beta_g / 4 \mu \omega. \quad (10)$$

Hence, the characteristic (circuit) impedance is found from Eq. (7), (8) and (10) to be

$$K_m = \sqrt{\mu/\epsilon} (2\omega l / c \beta_m^2 L^2 w \beta_g) \sin^2(\beta_m l/2) / (\beta_m l/2)^2, \quad (11)$$

where  $\sin(\beta_m l/2) / (\beta_m l/2)$  is the gap factor. The gap factor limits the bandwidth. From Eq. (11), it is seen that the impedance decreases as the space harmonic number  $m$  (i.e.  $\beta_m$ ) increases.

#### IV. INTERACTION IMPEDANCE AND GAIN

As mentioned earlier, the interaction impedance and gain of the spiraled waveguide amplifier are calculated on the basis of Pierce small signal theory [Ref. 3]. In this theory, the interaction impedance or so-called  $C^3$  parameter is defined by [Ref. 3]

$$C^3 = K_m l / 4 V_b, \quad (12)$$

where  $V_b/I$  is the beam impedance.  $V_b$  is the beam voltage and  $I$  is the current. By substituting Eqs. (12) and (4) into the modified Pierce formula [Ref. 3], the beam-wave dispersion relation may be written as

$$(\beta^2 - \beta_m^2) [(\beta - \omega/v_b)^2 - \beta_q^2] + 2\beta^2\beta_m\omega C^3/v_b = 0, \quad (13)$$

where

$$\beta_m = \beta_0 + 2\pi m/L - j\alpha = (\omega L/cL) \sqrt{1 - \omega_c^2/\omega^2} + \frac{2\pi m}{L} - j\alpha, \quad (14)$$

$$\alpha = (\epsilon\omega/2\sigma)^{1/2} (1 + 2l\omega_c^2/\omega\omega^2)/(\omega\sqrt{1 - \omega_c^2/\omega^2}), \quad (15)$$

$$\beta_q^2 = (4QC) \beta^2 C^2. \quad (16)$$

The quantity  $QC$  is the space charge parameter and  $\sigma$  is the conductivity of the waveguide wall. The definition of  $\beta_m$  is generalized to include the effect of losses in the circuit. Equation (13) is quartic in  $\beta$  and has four roots of  $\beta$  for a given frequency. One of these roots represents a backward wave and the other three are forward waves. Therefore, the dispersion characteristics for both the forward and the backward waves are obtained from Eq. (13). For a given angular frequency  $\omega$ , the gain is calculated from the imaginary part of  $\beta$ , ( $\text{Im}(\beta)$ ), obtained by solving Eq. (13). The gain per cm is given by

$$g = 20(\log_{10} e) \text{Im}(\beta) \text{ db/cm}. \quad (17)$$

The wave vector is given by the real part of  $\beta$  and the wavelength,  $\lambda = 2\pi/\text{Re}(\beta)$ .

Approximate solutions of  $\beta$  for the three forward waves may be written as [4]

$$\beta_1 = \beta_e \left[ 1 + \frac{C}{2} \right] + i \frac{\sqrt{3}}{2} \beta_e C, \quad (18)$$

$$\beta_2 = \beta_e^*,$$

$$\beta_3 = \beta_e (1 - C),$$

where  $\beta_e = \omega/v_b$  and  $C$  is the Pierce C-parameter. The root  $\beta_1$  represents the forward amplifying wave. The growth rate (i.e.  $\text{Im}(\beta)$ ) is proportional to the C-parameter. We calculate the real and imaginary parts of  $\beta$  numerically from Eq. (13). The total gain over an interaction length containing  $N$  wavelengths is given by

$$G(\text{dB}) = 40\pi N (\log_{10} e) \text{Im}(\beta) / \text{Re}(\beta). \quad (19)$$

This is known as the BCN gain.

Initially the electrons couple to all the four waves obtained from the dispersion relation Eq. (13). Neglecting the backward wave, the input power will be shared by the three forward waves at  $z = 0$ . The initial amplitudes of the three waves can be determined by applying the following boundary condition at  $z = 0$

$$\begin{aligned} \sum_{i=1}^3 E_i &= E_{in} \\ \sum_{i=1}^3 v_{1i} &= 0 \\ \sum_{i=1}^3 j_{1i} &= 0 \end{aligned} \quad (20)$$

where  $E_{in}$  is the electric field amplitude of the input signal and  $E_i$ ,  $v_{1i}$  and  $j_{1i}$  denote, respectively, the amplitudes, the velocity modulation and the current modulation of the three forward waves. Following Pierce's theory [4], it can be shown that Eq. (20) becomes

$$\begin{aligned} \sum_{j=1}^3 E_j &= E_{in} \\ \sum_{j=1}^3 \frac{E_j}{\zeta_j} &= 0 \\ \sum_{j=1}^3 \frac{E_j}{\zeta_j^2} &= 0 \end{aligned} \quad (21)$$

where  $\zeta_j = \beta_e - \beta_j$ .  $\beta_j$  are the roots of Eq. (13). If  $\beta_1$  denotes the root for the amplifying wave, then from Eq. (21), we have

$$E_i(z=0) = E_{in} \xi_1 \quad (22)$$

where

$$\xi_1 = \frac{(\zeta_1^2 - \zeta_p^2)(\zeta_2 - \zeta_3) \left\{ 1 + \zeta_p^2 / \zeta_2 \zeta_3 \right\}}{(\zeta_1^2 - \zeta_p^2)(\zeta_2 - \zeta_3) \left\{ 1 + \frac{\zeta_p^2}{\zeta_2 \zeta_3} \right\} + (\zeta_2^2 - \zeta_p^2) \left\{ 1 + \frac{\zeta_p^2}{\zeta_3 \zeta_1} \right\} (\zeta_3 - \zeta_1) + (\zeta_3^2 - \zeta_p^2)(\zeta_1 - \zeta_2) \left\{ 1 + \frac{\zeta_p^2}{\zeta_1 \zeta_2} \right\}} \quad (23)$$

and

$$\zeta_p^2 = \omega_p^2 / v_b^2 \quad (23a)$$

$E_2$  and  $E_3$  can similarly be obtained by permuting the indices 1,2,3 in Eq. (23). If the space charge effects are neglected ( $\zeta_p^2 = 0$ ), then

$$\begin{aligned} \xi_1 &= \frac{(\zeta_2 - \zeta_3) \zeta_1^2}{\zeta_1^2 (\zeta_2 - \zeta_3) + \zeta_2^2 (\zeta_3 - \zeta_1) + \zeta_3^2 (\zeta_1 - \zeta_2)} \\ &\approx 1/3 \text{ [if Eq. (18) is used for } \beta_1, \beta_2 \text{ and } \beta_3]. \end{aligned}$$

If the helix is long enough for the amplified wave to be much bigger than the other waves, then the gain in decibel is

$$\begin{aligned} G_T &= 20(\log_{10} e) \ln (\xi_1 e^{\beta_1 N_A}) \\ &= 20(\log_{10} e) \ln \xi_1 + G, \end{aligned} \quad (24)$$

where the first term in Eq. (24) denotes the insertion loss and  $G$  is given in Eq. (19). If the approximate value of  $\xi_1 \approx 1/3$  is used, then the insertion loss is  $-9.54$  dB.

## V. START OSCILLATION CURRENT

The backward wave oscillation is a common problem in the high power tube. This is caused by two different mechanisms. One is caused by the reflection at the tube end due to impedance mismatch (external feedback). Another is excited by itself due to the high current operation above the threshold current or start oscillation current (internal feedback). The external feedback is avoided when the product of two reflection coefficients at two ends of the tube,  $\rho_1$  and  $\rho_2$ , satisfies

$$(\rho_1 \rho_2)^{-1} > \text{the total gain.}$$

The internal feedback of the backward wave oscillator (B.W.O.) is discussed in detail in Ref. [5]. The gain of BWO becomes infinite for certain values of  $CN$  which is the condition for the tube to start oscillating. The oscillation conditions are found by setting the ratio of the electric field at the tube end to that at the gun end equal to zero. The resulting equation is

$$e^{i\zeta_1} \frac{(\zeta_3 - \zeta_2)}{\zeta_1} + e^{i\zeta_2} \frac{(\zeta_1 - \zeta_3)}{\zeta_2} + e^{i\zeta_3} \frac{(\zeta_2 - \zeta_1)}{\zeta_3} = 0. \quad (25)$$

where  $\zeta_i$ 's satisfies the cubic form of the dispersion equation (13)

$$\zeta^3 + 2\theta\zeta^2 + (\theta^2 - H^2)\zeta + (2\pi CN)^3 = 0 \quad (26)$$

Here

$$\zeta = (\beta_m - \beta) L \quad (27)$$

$$\theta = (\omega/v_b - \beta_m) L$$

$$H = \beta_q L$$

The phase parameter  $\theta$  in Eq. (27) is real but  $\zeta$  can be complex when  $\beta_m$  includes the wall loss term. For a lossless guide ( $\alpha = 0$  in Eq. 14), Eq. (25) and (26) yields a solution for the lowest threshold current

$$\begin{aligned} \theta_1 &= -3.002993 \dots \\ (CN)_1 &= 0.31405512 \dots \end{aligned} \quad (28)$$

when the space charge effects are neglected. This lowest threshold condition occurs at the smallest value of synchronization when  $\theta \approx -\pi$ . Higher threshold conditions are found near  $\theta \approx -(2n+1)\pi$  i.e.  $\theta_2 = -9.86$  and  $(CN)_2 = 0.588$ , etc. Higher threshold current can occur below and above the frequency for the lowest oscillation threshold current. We can rewrite the relationship for the start oscillation current in terms of the backward wave circuit impedance ( $K_m$ ), current and voltage,

$$I_s = (CN)_1^3 \cdot 4V_b/K_m N^3 \quad (29)$$

with the value of  $(CN)_1$  given in Eq. (28). The value of  $(CN)_1$  will slightly increase if the space charge effects and the circuit losses are included in the calculation. Instead of finding the start oscillation current ( $I_s$ ) for a specified circuit length, it is more convenient to calculate  $N_s$  (the threshold circuit length expressed in units of the wavelength) for a given operating current ( $I_b$ ). Since  $\text{Im}(\beta)$  i.e. the gain per unit length  $g$  in Eq. (17) is proportional to  $I^{1/3}$  and  $N_s$  in Eq. (29) is proportional to  $I^{-1/3}$ , the maximum attainable gain,  $gN_s\lambda$ , in the circuit (if backward wave oscillations are not prevented) is independent of the current. The threshold current ( $I_s$ ) for a particular circuit length ( $N$ ) can be obtained from the relation

$$I_s = I_b (N_s/N)^3. \quad (30)$$

In the examples given in the next section, we choose  $I_b = 1A$  as the operating current and calculate the corresponding value of  $N_S$ .

## VI. RESULTS AND DISCUSSIONS

The dispersion equation of the "empty" waveguide should be first carefully examined in order to find a proper circuit of interest. For this purpose, we rewrite the dispersion Eq. (4) in the following form,

$$(\omega/\omega_c)^2 = 1 + (\beta_m/\beta_c - 2\pi m/\beta_c L)^2 L^2/L_0^2 \quad (31)$$

where  $\beta_c \equiv \omega_c/c$  ( $= \pi/w$ ).

Since the large bandwidth is achieved usually near the grazing condition in which the beam line ( $\omega = \beta_m v_b$ ) and the waveguide dispersion curve are tangential, we first find the circuit parameters at this grazing point ( $\omega_{0g}, \beta_{m0}$ ), where

$$\omega_0/\omega_c = (\beta_{m0}/\beta_c)/(v_b/c) \quad (32)$$

$$\beta_{m0}/\beta_c = [(2mw/L)^2 + L_0^2/L^2]/(2mw/L) \quad (33)$$

$$L/L_0 = (v_b/c)/[1 - (v_b^2/c^2)(2mw/L)^2]^{1/2}. \quad (34)$$

The gain at the grazing condition can easily be estimated from the dispersion relation of (13) for the beam-wave interaction. The gain per period at this point is

$$\begin{aligned} \text{gain/period} &= 20 (\log e) (\omega/v_b) LC \sqrt{3}/2 \\ &= 23.63 (\omega/\omega_c) (L/w) (c/v_b) C. \end{aligned} \quad (35)$$

Due to the linear dependency of gain on the Pierce  $C$ -parameter, the argument  $\beta_m l/2$  of sine function of  $K_m$  in Eq. (11) should be chosen to avoid the minimum in the impedance and the gain. Hence,  $\beta_m l$  should lie in the range

$$2\pi n < \beta_m l < 2\pi (n + 1) \quad (36)$$

where  $n$  is an integer.

The efficiency  $\eta$  (the RF output power/beam power) is estimated as in the linear beam tubes approximately by the formula

$$\eta \approx 2C. \quad (37)$$

Experimental values of efficiency usually fall in the range  $C \leq \eta \leq 3C$ . The value of the Pierce parameter  $C$  decreases as  $m$  increases. For  $m = 1$ , the value of  $C$  is found to be  $\sim 0.0215$ . Thus, the efficiency is estimated to lie in the range 2.2 to 6.5%.

Ideally, one would like to obtain the circuit and the beam parameters for a desired performance characteristic. The theory, on the other hand, calculates the performance characteristics of the circuit for a given set of the circuit and the beam parameters. Thus, a large number of data are generated by varying all the relevant parameters and the desired performance characteristic is found. In this report, we show some selected data which will bring out the essential features of this circuit. First, we present the results calculated with the design parameters originally proposed in Ref. [2]. The circuit parameters are  $L = 2$  cm,  $l = 0.127$  cm,  $w = 0.254$  cm and  $R_0 = 1.11$  cm. The beam current is 1 A and the beam voltage lies between 10.0 kV and 10.4 kV. At these values of the voltage, the waves with the space harmonic number  $m = 12$  satisfy resonance condition with the beam line. The dispersion curve for the forward waves in the empty waveguide are shown together with the beam line in Fig. 2. The grazing condition for this case is found from Eqs. (32-34) to be  $\beta_{12,0} \approx 187.75$ ,  $\omega/\omega_c = 1.51$  and  $v_0/c \approx 0.1995$ . The gain and the impedance of the circuit are shown in Figs. 3 and 4, respectively. The maximum gain changes from 0.54 dB/cm to 0.74 dB/cm and the bandwidth decreases from 15% to 5% as the voltage is increased from 10.2 kV to 10.4 kV. The gain vanishes at the frequency  $\omega/\omega_c \approx 1.58$  where the gap factor becomes zero. The forward wave dispersion curve for  $m = 12$  is intersected by many backward waves ( $m = 34$  to  $m = 64$ ) within the frequency range of interest as shown in Fig. 5. The backward waves have narrow bandwidth and the gain is about 1.2 dB/cm which is higher than the gain of the forward waves. The gain as a function of frequency is shown in Fig. 6 for two backward waves ( $m = 34$  and  $m = 44$ ). Since the performance of the circuit considered above is limited, the experiment [2] will be performed with a different set of parameters.

The gain and the bandwidth can be greatly improved by operating with the low order space harmonics. The best overall performance is obtained with the  $m = 1$  mode. The low order modes are more advantageous e.g., the number of backward waves in the useable frequency band is smaller and the ratio of the backward wave to forward wave gains is also lower. We discuss below the characteristics of all the space harmonics from  $m = 0$  to  $m = 4$ . In all these cases, the operating current is 1 A,  $w = 1.58$  cm and  $l = 0.203$  cm. The pitch ( $L$ ) and the radius ( $R_0$ ) of the helix and the beam voltage

( $V_b$ ) are chosen in each case so that the beam line is nearly tangential to the waveguide dispersion curve. The dispersion curves for the  $m = 3$  and  $m = 4$  modes together with the beam line are shown in Fig. 7. The circuit parameters  $L = 3.6$  cm and  $R_0 = 2.068$  cm are the same for both the modes but  $V_b = 12.7$  kV and 10.1 kV, respectively, for  $m = 3$  and  $m = 4$ . The gain as a function of frequency for  $m = 4$  mode is shown in Fig. 8 at values of  $V_b$  ranging from 9.9 kV to 10.3 kV. The gain and the bandwidth are sensitive functions of  $V_b$ . At higher  $V_b$ , the two intersection points of the beam line and wave dispersion curves are well separated and the gain shows two peaks near these intersections. As  $V_b$  is lowered, the two intersection points approach each other and finally coalesce when the beam line is tangential to the wave dispersion curve. Correspondingly, the two peaks in the gain curve merge into a single peak. The peak forward wave gain for  $m = 4$  mode is 0.96 dB/cm (0.472 dB/wavelength) at  $\omega/\omega_c = 1.31$ . If the backward waves are neglected, then the bandwidth is 20% ( $1.21 < \frac{\omega}{\omega_c} < 1.48$ ) for a total gain of 30 dB attained in an interaction length containing 65.87 wavelengths. Such a high gain may not be realized in practice due to the onset of oscillations. The frequency range  $1.17 < \frac{\omega}{\omega_c} < 1.75$  in the  $m = 4$  mode is intersected by 10 backward waves with mode numbers ranging from  $m = 9$  to  $m = 18$ . The peak backward wave gain is 0.924 dB/cm and occurs with  $m = 10$  mode at  $\omega/\omega_c = 1.21$ . The lowest threshold interaction length (expressed in number of wavelengths) is  $N_s = 29.34$ . Therefore, the maximum forward wave gain attainable is 13.4 dB if the backward wave oscillation cannot be suppressed. At this low gain, the bandwidth is 39.7%. This is the only mode found where the backward wave gain is slightly lower than the forward wave gain. The peak gain could be increased by operating at higher  $V_b$  but the bandwidth will decrease.

The gain as a function of frequency for  $m = 3$  mode is shown in Fig. 9. The peak gain is 0.83 dB/cm (0.367 dB/wavelength) at  $\omega/\omega_c = 1.57$  with  $V_b = 12.7$  kV. The bandwidth is 29% in the frequency range  $1.42 < \frac{\omega}{\omega_c} < 1.91$  for a total gain of 30 dB with an interaction length  $N = 81.76$ . The oscillations have to be avoided to obtain 30 dB gain since the lowest threshold is  $N_s = 36.75$  at  $\omega/\omega_c = 1.45$  (see Table II). This interaction length corresponds to a forward wave gain of 13.49 dB and the bandwidth at this level of gain is 42% ( $1.35 < \frac{\omega}{\omega_c} < 2.07$ ). The lowest threshold occurs with the  $m = 12$  backward wave mode and the peak backward wave gain is 0.834 dB/cm at  $\omega/\omega_c = 1.45$ . The number of the backward wave modes excited in the frequency band  $1.35 < \frac{\omega}{\omega_c} < 2.1$  is 8.

The gain and the bandwidth are further increased for the  $m = 1$  and  $m = 2$  modes. In these cases, circuits with shorter pitch and smaller radius are chosen to keep the operating voltage below 12



kV. The parameters for  $m = 2$  mode are  $L = 2.0$  cm,  $R_0 = 1.135$  cm and  $V_b = 11.3$  kV. The dispersion and the gain are shown in Figs. 10 and 11, respectively. The peak forward wave gain is 1.39 dB/cm (0.685 dB/wavelength) at  $\omega/\omega_c = 1.32$  and the peak backward wave ( $m = 5$ ) gain is 1.45 dB/cm at  $\omega/\omega_c = 1.17$ . The lowest threshold for oscillation is  $N_s = 18.13$  and this limits the total forward wave gain in the circuit to 12.4 dB. The bandwidth at this gain is 52% in the frequency band  $1.14 < \frac{\omega}{\omega_c} < 1.94$ . The number of backward waves in this frequency range is 6 from  $m = 5$  to  $m = 10$ . If the backward waves are suppressed, then a 30 dB gain is obtained in an interaction length of  $N = 43$ . The corresponding bandwidth is 30%.

For  $m = 1$  mode, the parameters chosen are  $L = 1.0$  cm,  $R_0 = 0.616$  cm and  $V_b = 10.2$  kV. The gain is shown in Fig. 12 as a function of frequency. The peak forward wave is found to be 2.17 dB/cm at  $\omega/\omega_c = 1.35$ . The peak backward wave gain is 2.24 dB/cm at  $\omega/\omega_c = 1.26$  for  $m = 3$  backward wave and lowest threshold for oscillation  $N_s = 13.27$ . Thus the limiting value of gain for  $m = 1$  mode is 13.2 dB assuming the backward wave are not suppressed. The bandwidth is 57% in the frequency range  $1.09 < \frac{\omega}{\omega_c} < 1.96$ . There are 4 backward waves ( $m = 3, 4, 5, 6$ ) in this frequency band. If backward waves are avoided, then a gain 30 dB can be achieved with a circuit length  $N = 30.2$ . The corresponding bandwidth is 36% in the frequency range  $1.15 < \frac{\omega}{\omega_c} < 1.65$ .

The fundamental mode ( $m = 0$ ) is not suitable for broadband operation. The phase velocity of this mode as a function of frequency is shown in Fig. 13. Similar curves for other modes are also included for comparison. As seen from Fig. 13, the grazing condition for the  $m = 0$  mode occurs at very high frequency and this leads to lower gain and bandwidth near cut-off. The pitch,  $L$ , of the helix becomes unreasonably small to maintain the beam-wave resonance if  $V_b$  is less than 12 kV. For this reason we choose  $V_b = 19$  kV,  $L = 0.8$  cm and  $R_0 = 0.493$  cm. With these parameters, the peak gain for the  $m = 0$  mode is 1.37 dB/cm (0.402 dB/wavelength) at  $\omega/\omega_c = 2.85$ . The peak backward wave ( $m = 4$ ) gain is 1.77 dB/cm at  $\omega/\omega_c = 2.16$  and the lowest oscillation threshold is  $N_s = 21.4$ . The maximum gain of the circuit in this interaction length is 8.62 dB. If the backward waves are suppressed, a gain of 30 dB can be achieved with  $N = 75$  and a bandwidth of 21% ( $2.47 < \frac{\omega}{\omega_c} < 3.05$ ). The number of backward waves in this frequency band is 3 with  $m = 4, 5$  and 6.

A comparison of the performance characteristics for the various space harmonics is shown in Table I. The backward wave properties are listed in Table II. An examination of Table I shows that the device performance is better for low order modes and the optimum performance is obtained with the  $m = 1$  mode.

## VII. CONCLUSION

We have developed a linear theory to calculate the gain and the bandwidth of the helical waveguide. The large diameter of the circuit permits the injection of a high current beam but the impedance and the gain are low. The development of this circuit as a broad-band and high gain amplifier will be difficult if the large number of backward waves cannot be suppressed. The backward wave gain is in general found to be higher than the forward wave gain in this circuit. The amplifier will operate better with low order modes. The forward wave gain and the bandwidth are larger for the low order modes. Also, the ratio of the backward to the forward wave gains and the number of the backward waves excited are smaller for the low order modes. For beam voltage in the range of 10 kV to 13 kV, the largest gain and bandwidth are obtained with  $m = 1$  mode. The peak gain is about 2.17 dB/cm and the bandwidth is 50% if the total gain is limited to 12 dB to avoid the onset of oscillations. Alternatively, if the backward wave oscillation can be suppressed, a total gain of 30 dB with 40% bandwidth could be obtained. For these conditions, the backward wave gain is 2.24 dB/cm. The ratios of the forward to the backward wave gains are 1.032 for  $m = 1$  and 1.6 for  $m = 12$  modes. The value of  $N_s$ , (the interaction length expressed in number of wavelengths) for the onset of oscillation is found to be 13.27 in the case of the  $m = 1$  mode. This limits the total gain of the circuit to about 12 dB. The same limit is also obtained for  $m = 2, 3$  and 4 modes.

The backward waves may be suppressed by tapering the interaction parameters. The easiest method is to taper the pitch of the helix. The circuit may, however, be used as a high power, high gain but narrow-band amplifier if the suppression of the backward wave oscillations is found to be difficult.

## VIII. ACKNOWLEDGMENT

We gratefully acknowledge useful discussion with Dr. S. Smith, Dr. R. Parker, Dr. R. Phillips and Mr. N. Vanderpleats on various aspects of the problem.

## IX. REFERENCES

- [1] R.A. Waldron, "Theory of the helical waveguide of rectangular cross-section," L. British I.R.E., p. 577, October (1957). This article contains dispersion analysis. Some general discussion is found in "Helical waveguides—closed, open and coaxial" by G.M. Clarke in p. 359 of J. British I.R.E., June (1958) together with the comment by Waldron. See also remarks in "Survey of structures having high power broadband potentialities," Report No. RF/265 by Pearce, prepared for C.V.D. Admiralty, England (May 1959). See also Tech. Rep. No. 458-1, Nov. 4, 1958 (Stanford Elect. Lab) by M. Disman.

- [2] S. Smith, et al., "The quest for inherently wide bandwidth amplifiers for mm wave applications," Quarterly Prog. Report NRL 5733-33 (June 4, 1982).
- [3] J.R. Pierce, "Traveling-wave Tubes," D. Van Nostrand Co., Inc., Princeton, NJ (1950).
- [4] R.G.E. Hutter, "Beam and wave electronics in microwave tubes," D. Van Nostrand Co., Inc., Princeton, NJ (1960).
- [5] H. Heffner, "Analysis of the Backward-Wave Traveling-Wave Tube," Proc. IRE, Vol. 42, pp. 930-937 (June 1954).
- [6] H.R. Johnson, "Backward-Wave Oscillators," Proc. IRE, Vol. 43, pp. 684-697 (June 1955).

TABLE I

$m$	$V_b$ (kV)	$g_f$ (dB/ $\lambda$ )	$g_b/g_f$	$N_s$	$G$ (dB)	$\Delta\omega/\omega$ (%)	$M_b$	$N$ (for 30 dB total gain)	$\Delta\omega/\omega$
0	19.0	0.56	1.3	21.4	8.6	—	3	75	21%
1	10.14	0.993	1.032	13.27	13.2	57%	4	30	36%
2	11.3	0.685	1.043	18.13	12.4	48%	6	43	30%
3	12.7	0.367	1.005	27.37	11.2	43%	9	82	29%
4	10.1	0.472	0.9625	29.34	13.4	38%	10	66	25%
12	10.2	0.04	1.6	—	—	—	31	750	15%

$m$  = forward wave mode number

$g_f$  = peak forward wave gain in dB per wavelength

$N_s$  = lowest threshold interaction length expressed in wavelengths

$\Delta\omega/\omega$  = bandwidth

$N$  = interaction length for 30 dB gain

$V_b$  = beam voltage

$g_b/g_f$  = backward wave gain/forward wave gain

$G$  = maximum forward wave gain in  $N_s$  wavelengths

$M_b$  = no. of backward waves in the frequency band  $\Delta\omega$

TABLE II

Mode No. $m$	Circuit Parameters and Beam Voltage	Backward wave mode ( $m$ )	Impedance (ohms)	Threshold ( $N_S$ )	Oscillation frequency/ cut-off-freq.	Backward wave gain (dB/cm)
$m = 1$	$L = 1$ cm $R_0 = 0.616$ cm $L/L_0 = 0.25$ $V_b = 10.2$ kV	6	0.0262	36.4	2.19	1.402
		5	0.0783	25.27	1.87	1.746
		4	0.2020	18.42	1.55	1.980
		3	0.5410	13.27	1.26	2.237
$m = 2$	$L = 2$ cm $R_0 = 1.136$ $L/L_0 = 0.27$ $V_b = 11.3$ kV	9	0.0309	35.64	1.80	1.128
		8	0.0496	30.44	1.63	1.207
		7	0.0805	25.90	1.47	1.250
		6	0.1320	21.97	1.31	1.341
		5	0.2350	18.13	1.17	1.450
$m = 3$	$L = 3.6$ cm $R_0 = 2.06$ cm $L/L_0 = 0.2675$ $V_b = 12.7$ kV	15	0.0147	47.47	1.73	0.7716
		14	0.0187	43.81	1.63	0.7950
		13	0.0244	40.15	1.54	0.8198
		12	0.0318	36.75	1.45	0.8420
$m = 4$	$L = 3.6$ cm $R_0 = 2.06$ cm $L/L_0 = 0.2675$ $V_b = 10.1$ kV	15	0.0119	47.19	1.63	0.7940
		14	0.0156	43.12	1.54	0.7947
		13	0.0208	39.18	1.46	0.8791
		12	0.0277	35.61	1.37	0.8800

(w = 1.58 cm,  $l = 0.203$  cm for all circuits listed in this table.)

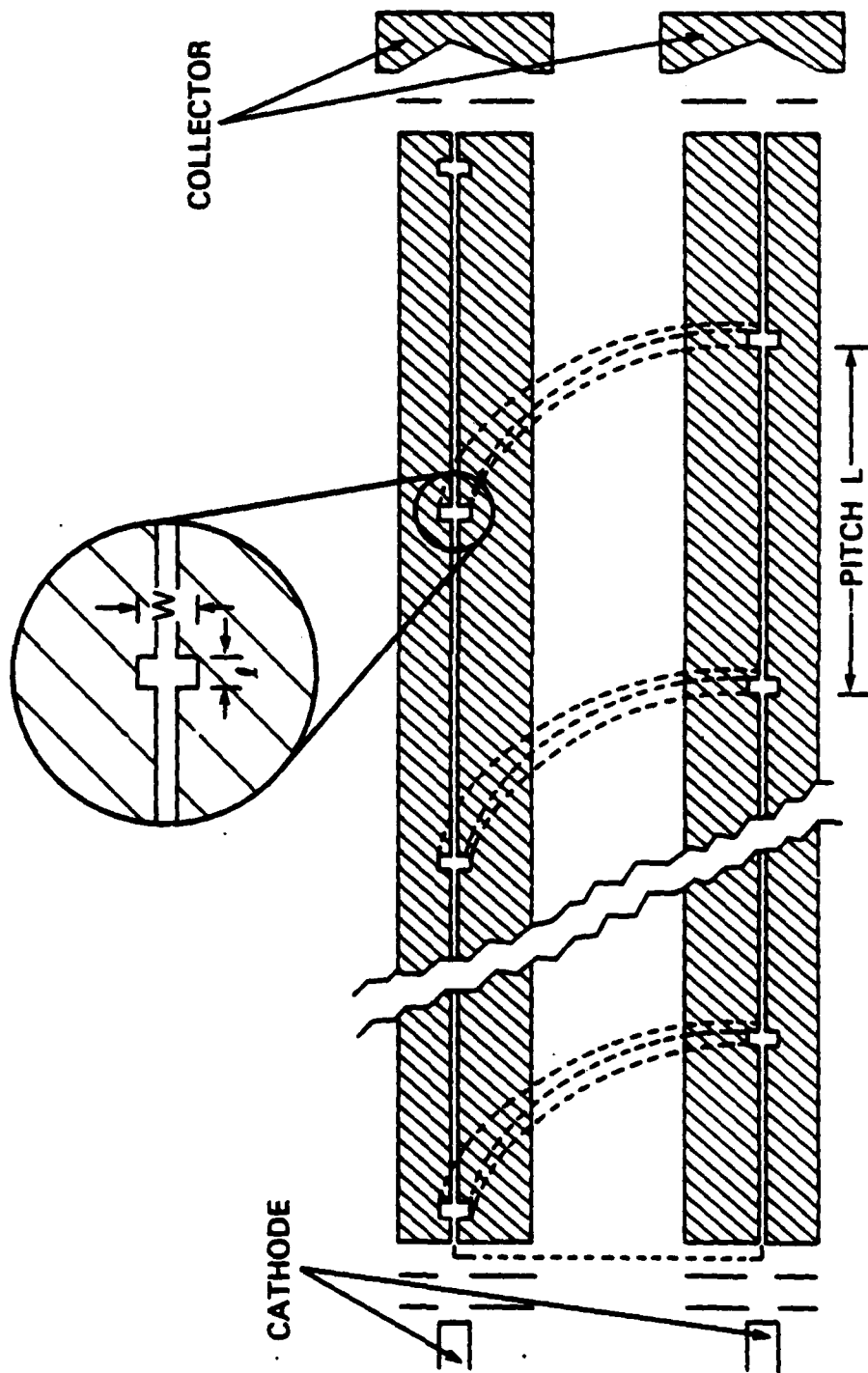


Fig. 1. Spiraled waveguide transmission line for the millimeter wave amplifier. The annular electron beam is generated by the Pierce type gun and injected into the annular shaped slit of the above waveguide. The r.f. wave coupled in the rectangular waveguide wall (not shown in this figure) travels around the spiraled waveguide with the pitch  $L$  and radius  $R_0$ . The collector is drawn schematically.

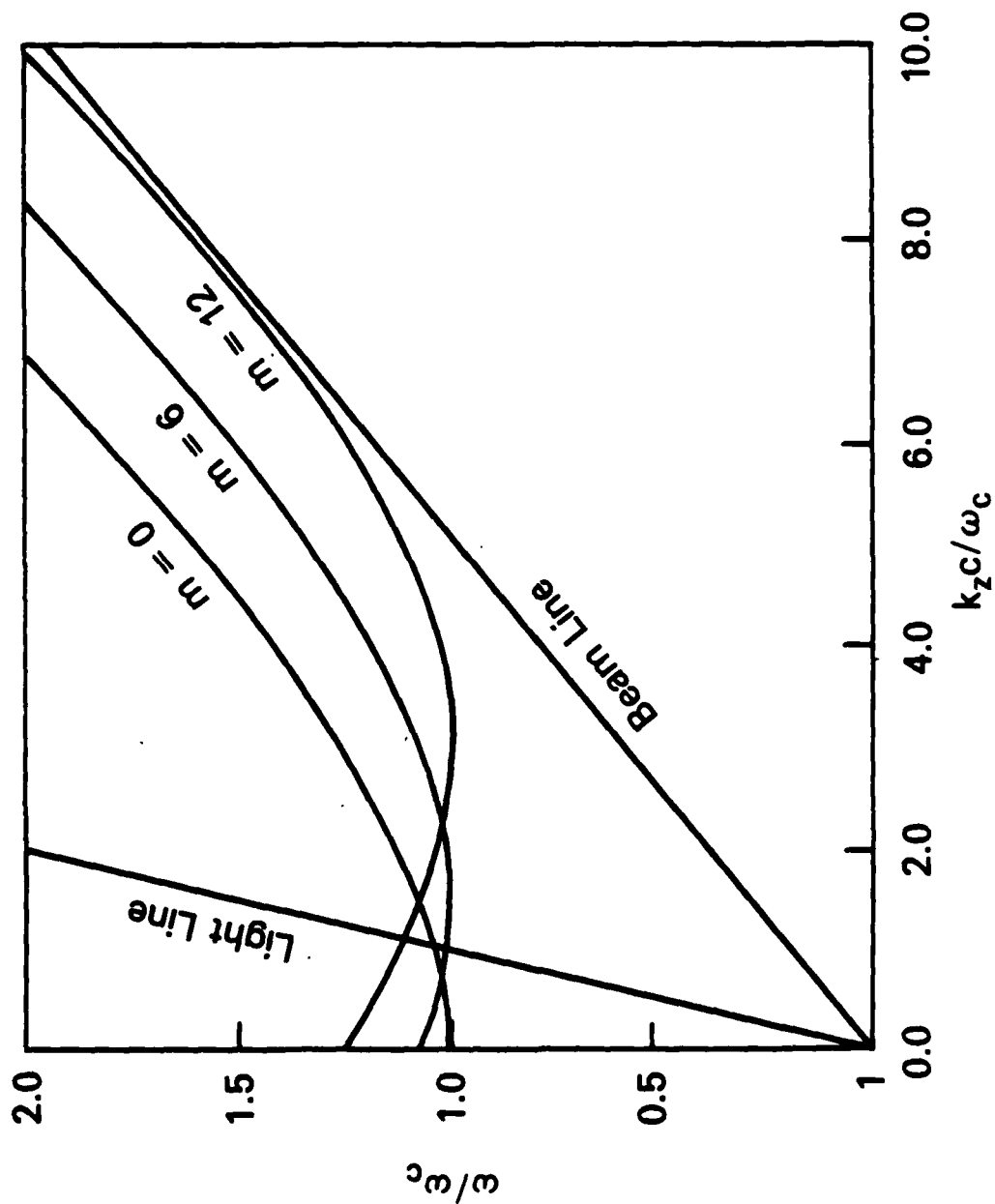


Fig. 2. The three space harmonics,  $m = 0, 6$  and  $12$ , of the forward wave are shown for the first case considered in Section VI together with the modes of electron beam and light wave in the free space. (Case 1)

# SPIRAL WAVEGUIDE : GAIN OF $m=12$ MODE

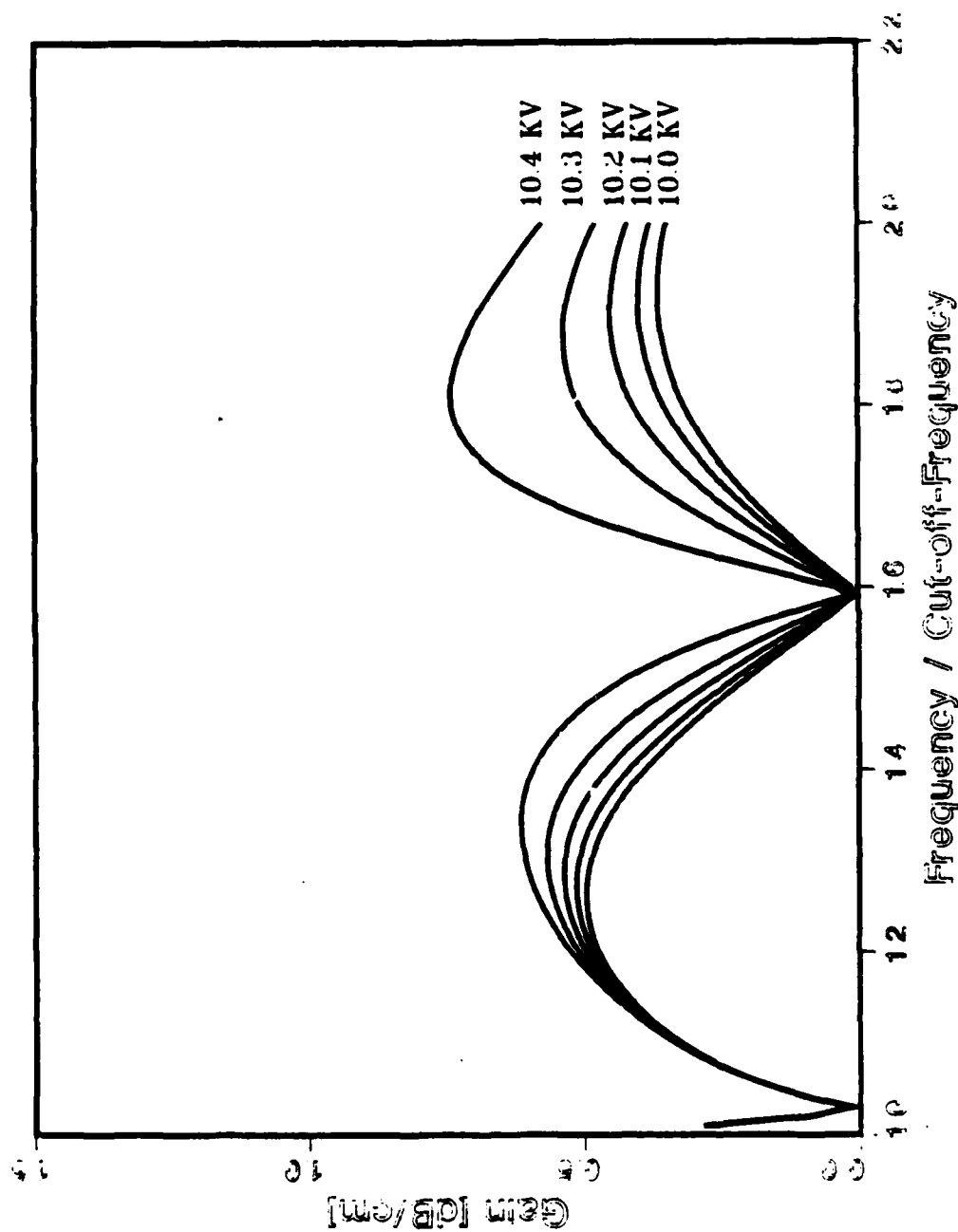


Fig. 3. The gain curves of the forward space harmonic  $m = 12$  are drawn for three different beam voltages  $V = 10.0, \sim 10.4$  kV



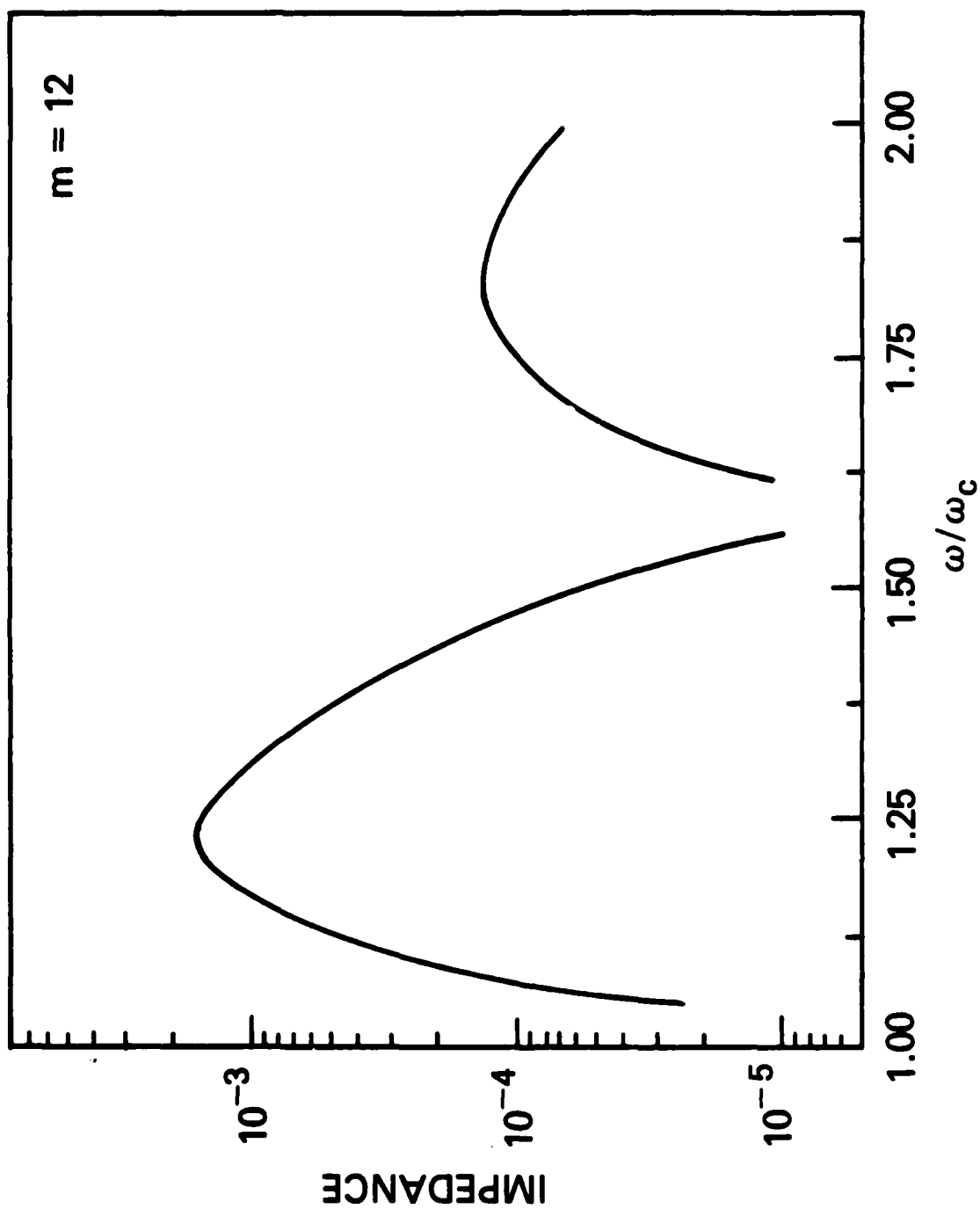


Fig. 4. The impedance of the empty waveguide for  $m = 12$  mode with  $V_0 = 10.1$  kV

# DISPERSION

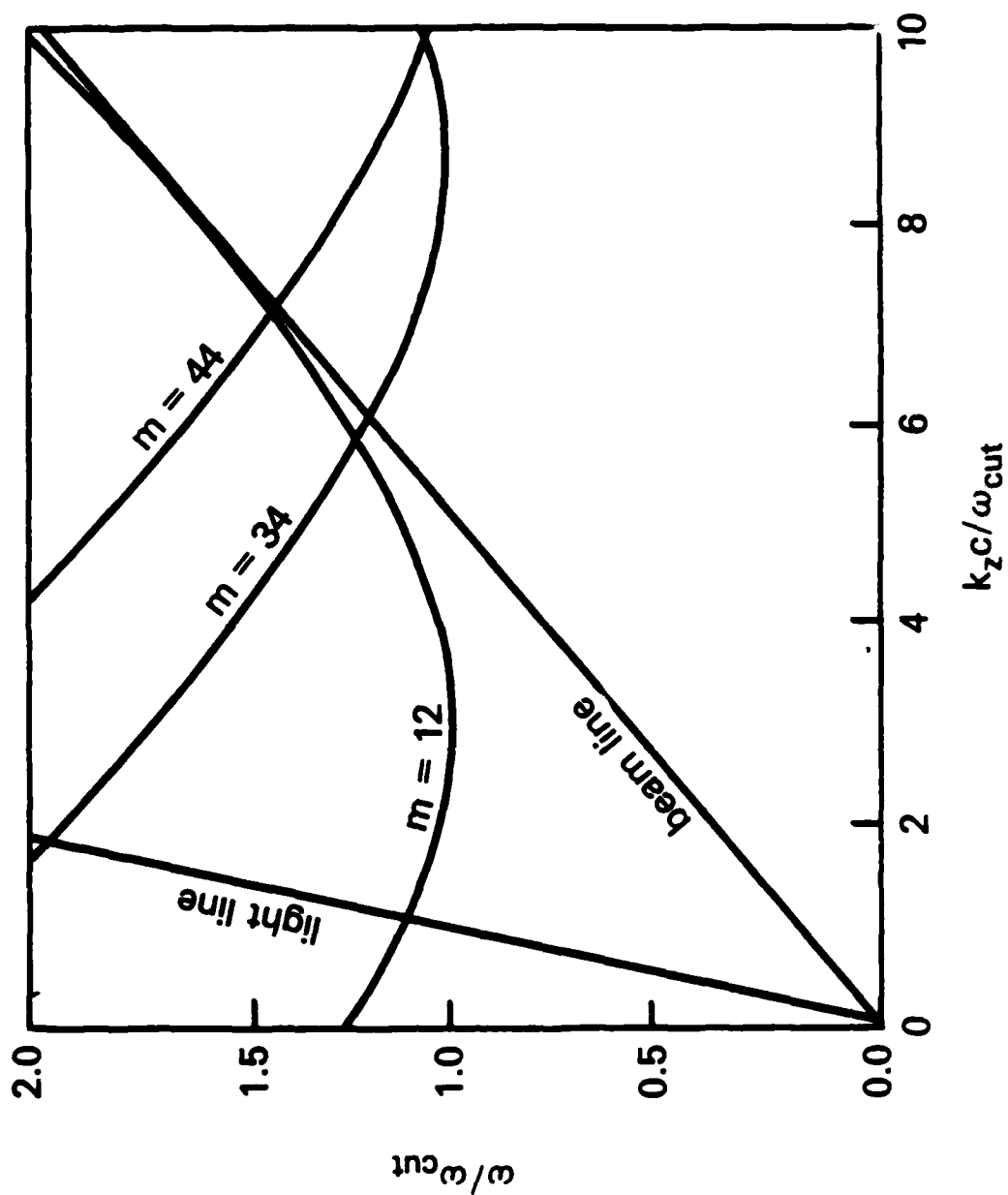


Fig. 5. Two representative backward waves are shown to cross the forward wave with  $m = 12$

# GAIN CURVE

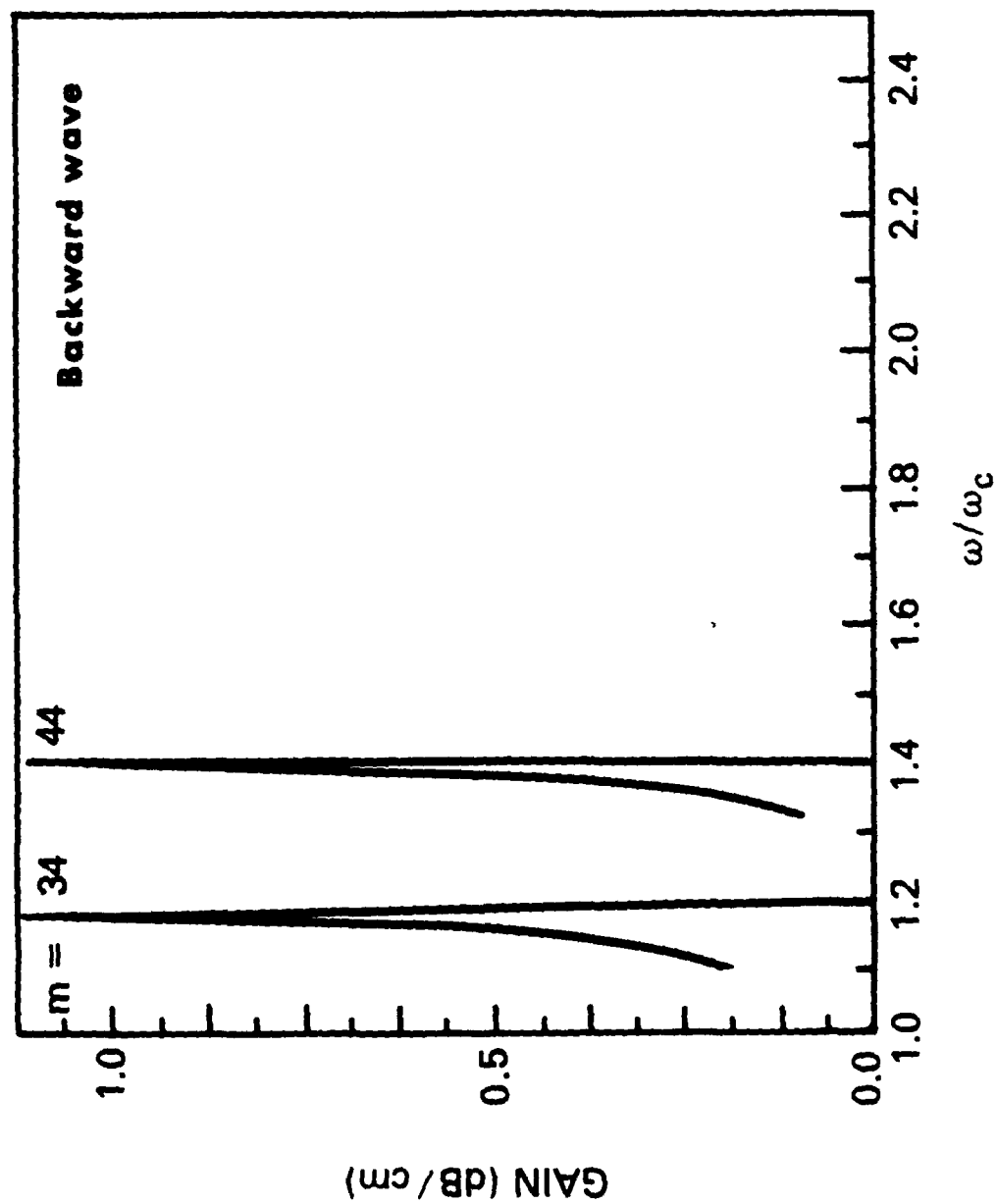


Fig. 6. Backward wave gains are shown for different space harmonics for the  $m = 12$  mode circuit with  $V_0 = 10.1$  kV

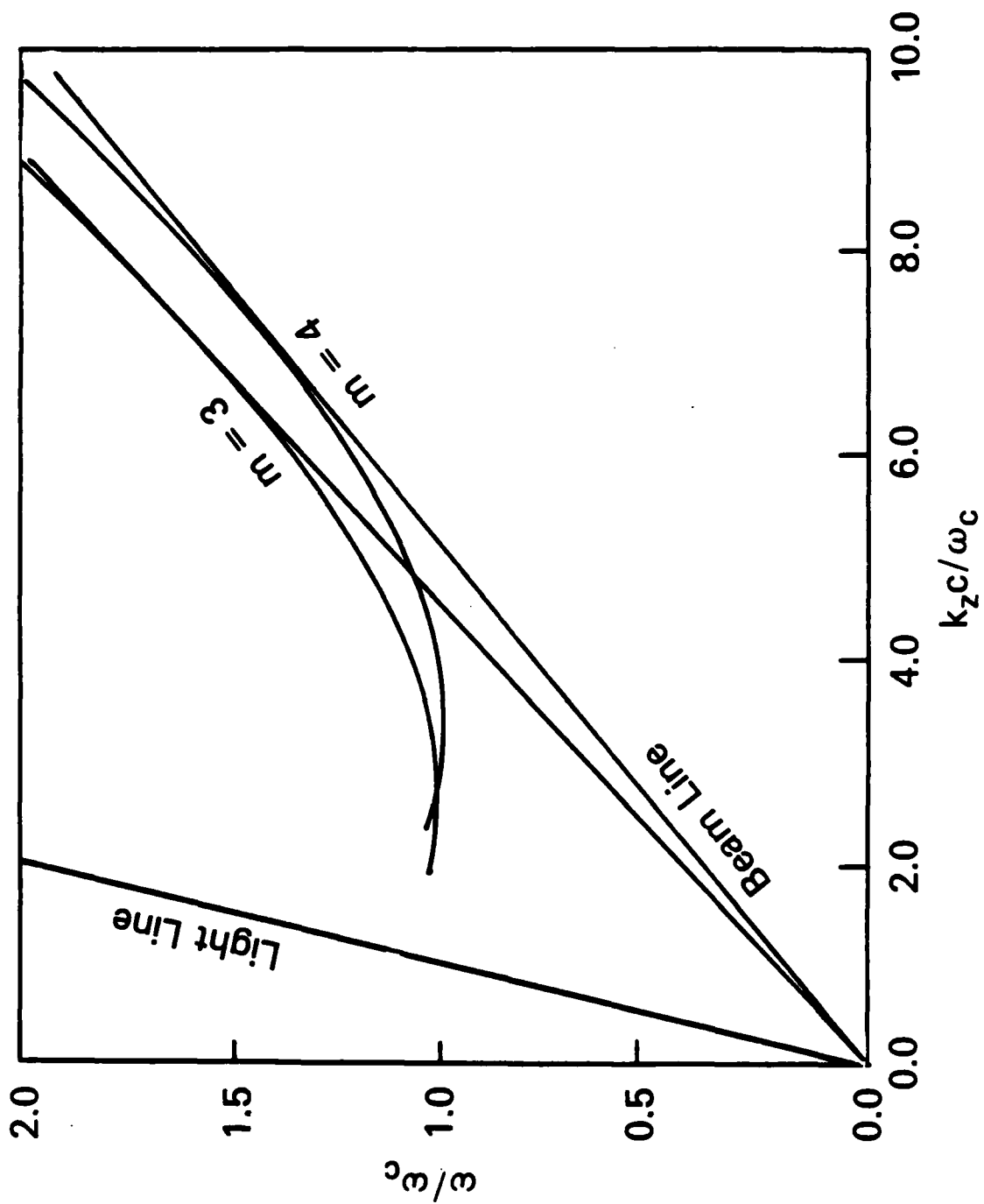


Fig. 7. Dispersion curves of the two space harmonics  $m = 4$  and  $m = 3$  are shown with the corresponding curves of tangential beam lines at  $V = 10.1$  and  $12.7$  kV respectively.

# SPIRAL WAVEGUIDE : GAIN OF $m=4$ MODE

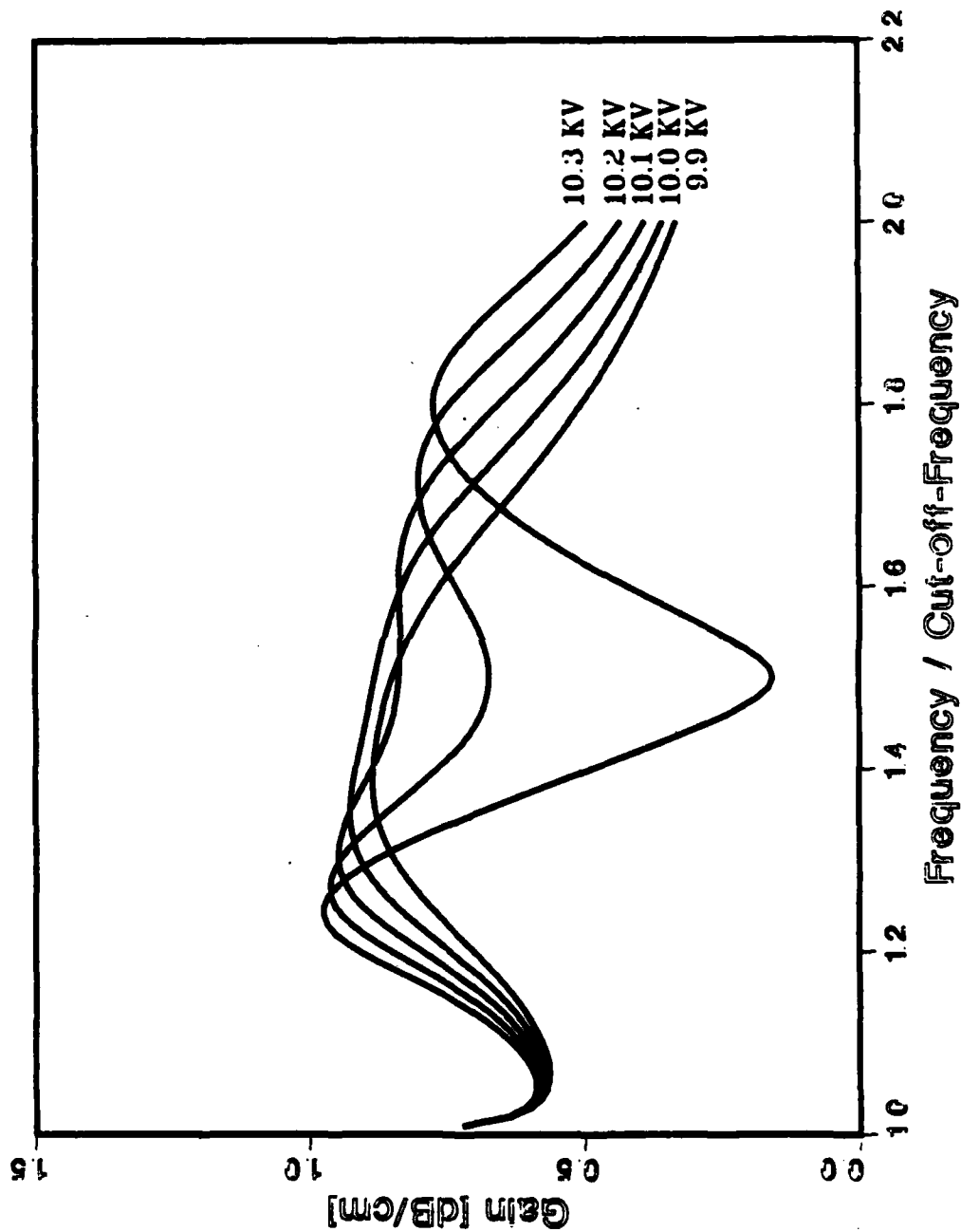


Fig. 8. The forward wave gains are shown for the  $m = 4$  mode with  $V = 9.9, \sim 10.3$  kV

# SPIRAL WAVEGUIDE : GAIN OF $m=3$ MODE

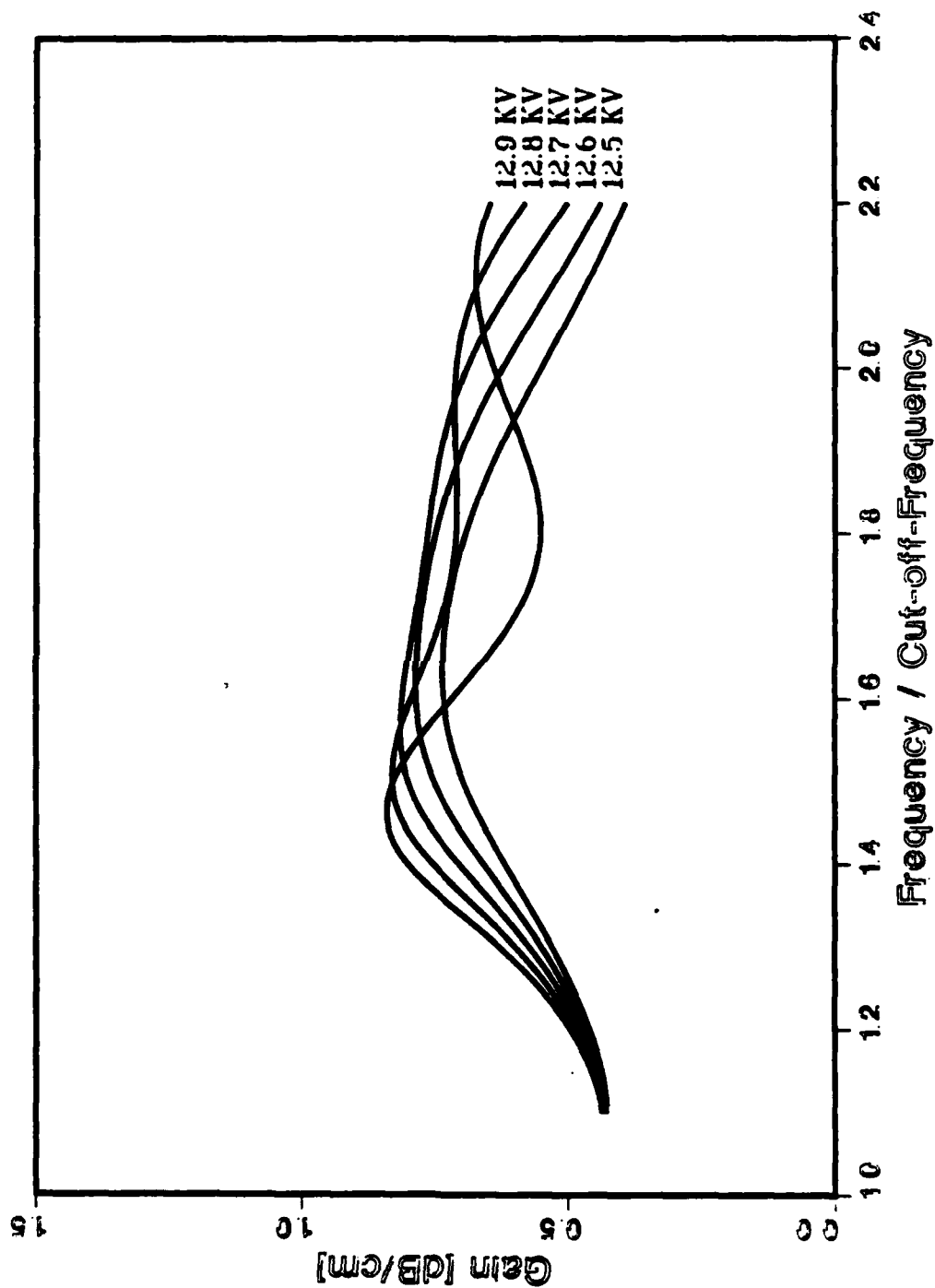


Fig. 9. The forward wave gains are shown for the  $m = 3$  mode with  $V = 12.5 \sim 12.9$  kV

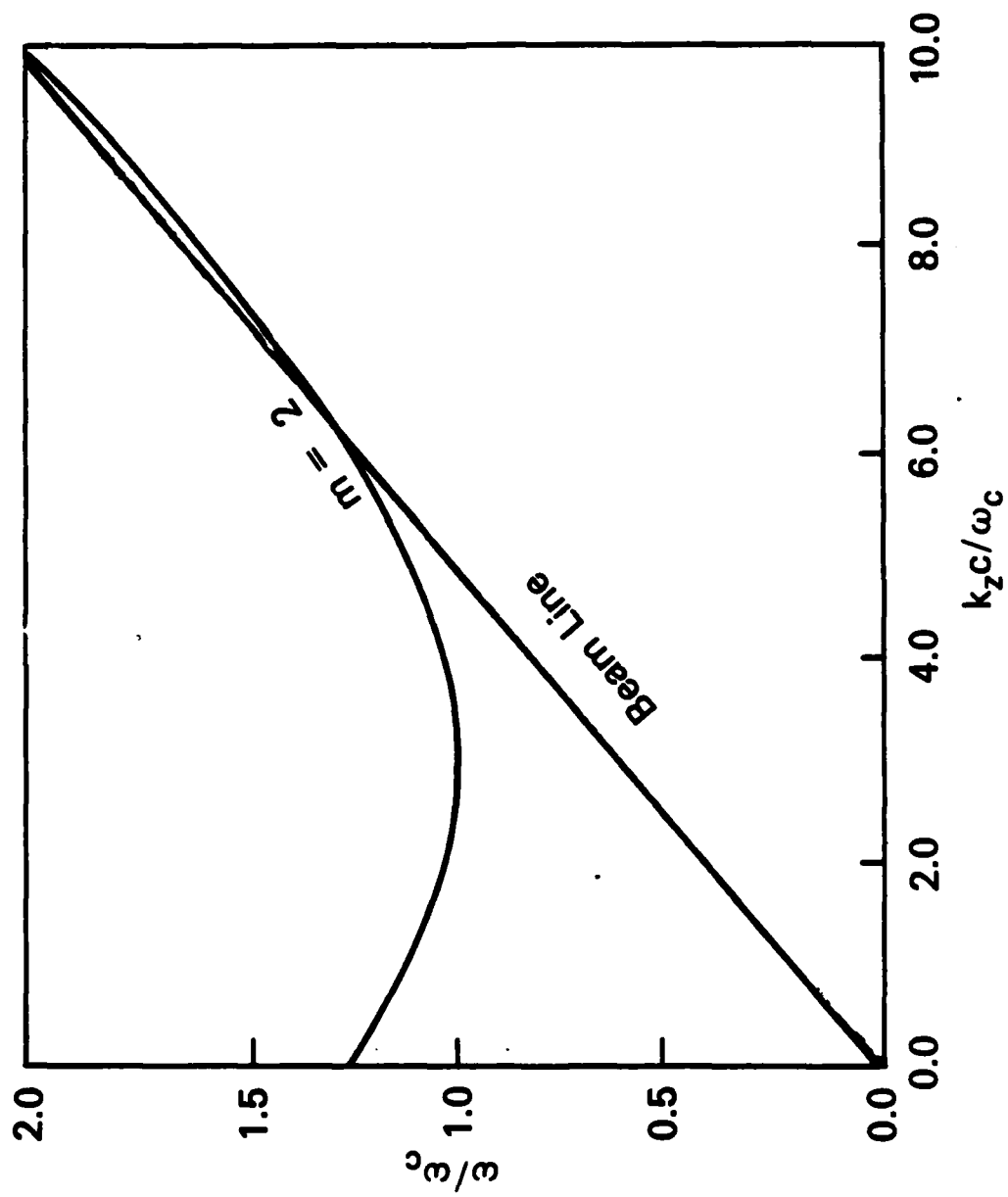


Fig. 10. The dispersion curve of the  $m = 2$  mode is drawn with the beam line

# SPIRAL WAVEGUIDE : GAIN OF $m=2$ MODE

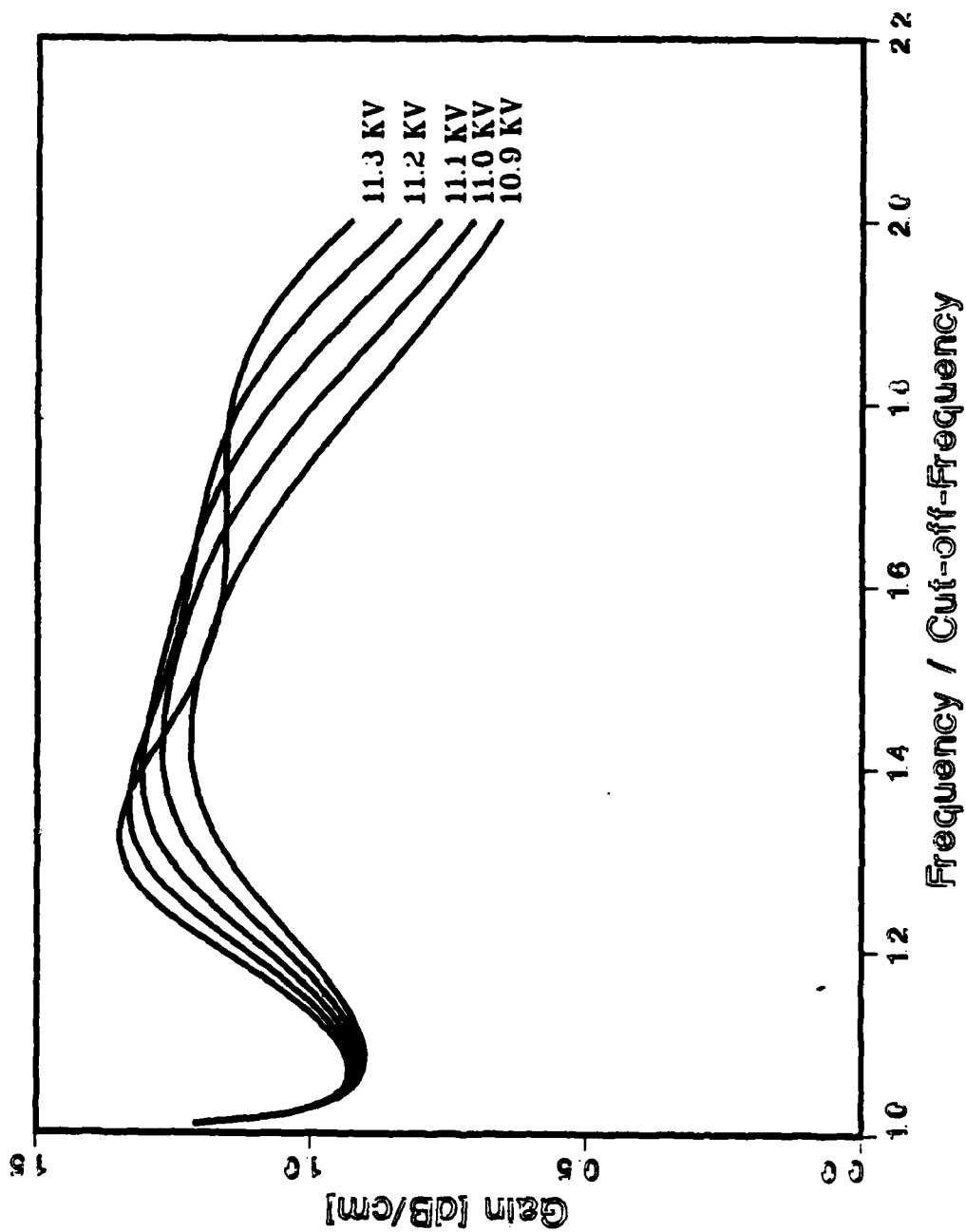


Fig. 11. The forward wave gains of the Case 4 are shown for the beam voltage  $V = 10.9 \sim 11.3$  kV respectively



# SPIRAL WAVEGUIDE : GAIN OF $m=1$ MODE

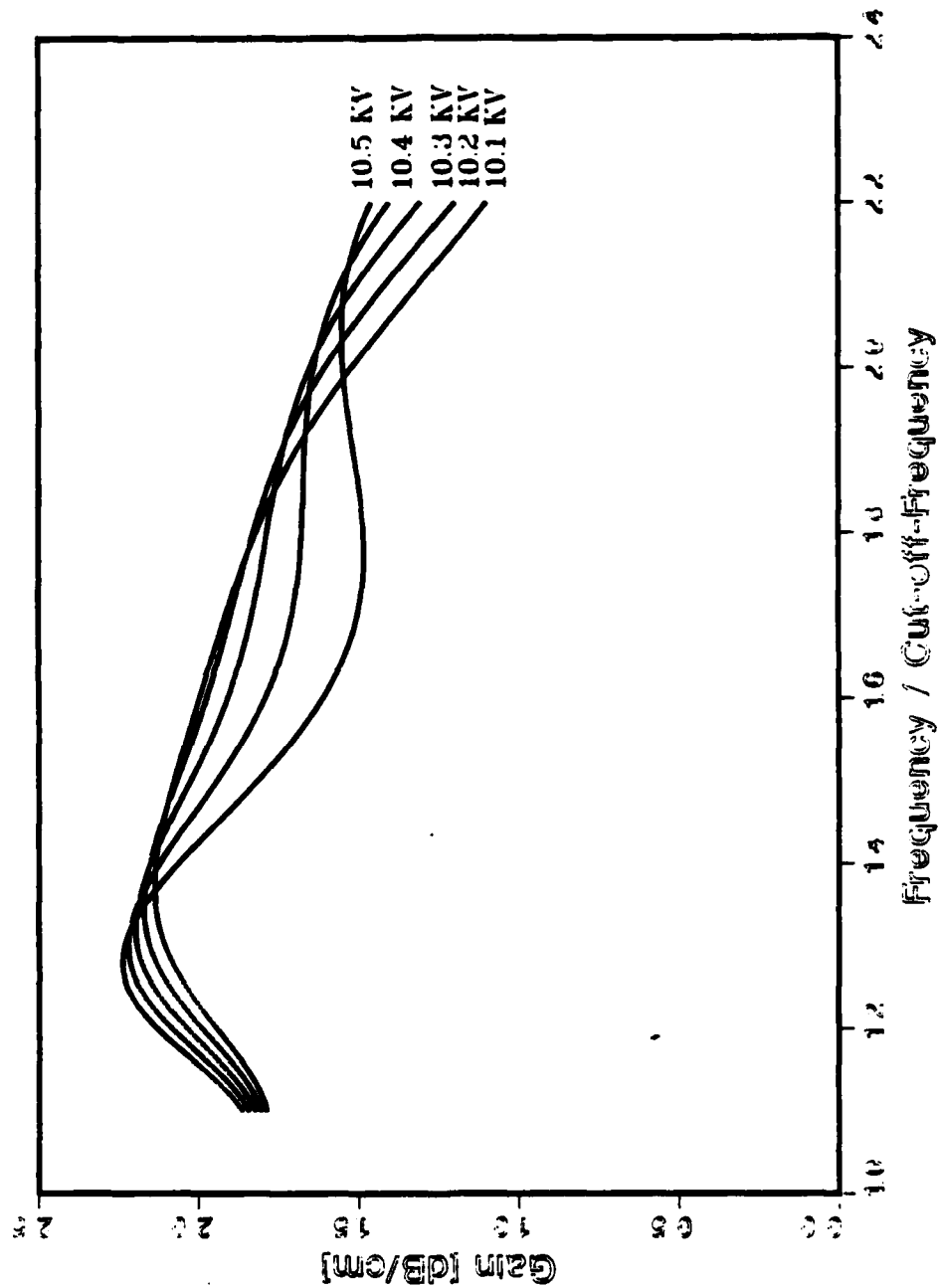


Fig. 12. Gain vs frequency for  $m = 1$  mode

# SPIRAL WAVEGUIDE : PHASE VELOCITY

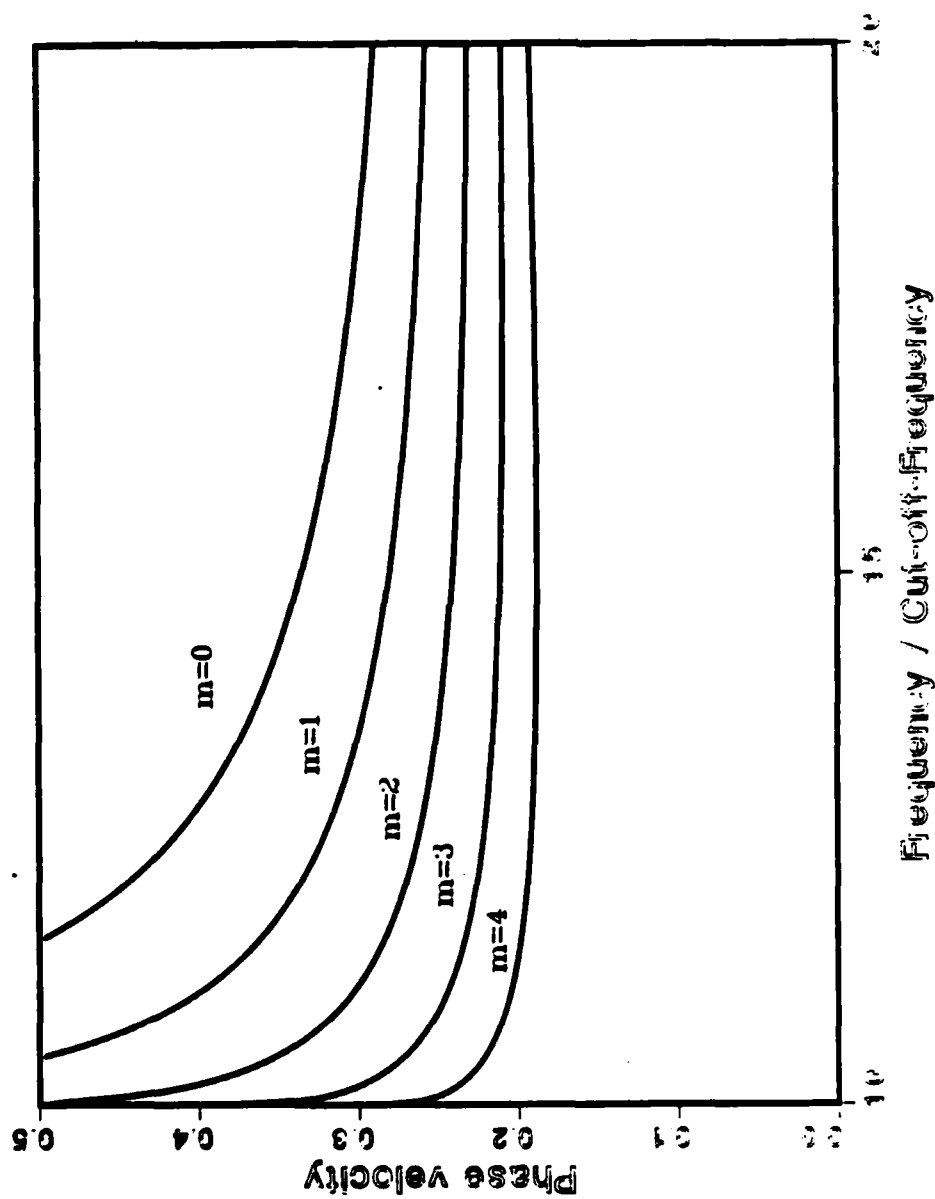


Fig. 13. Phase velocity vs frequency

**END**

**FILMED**

**2-86**

**DTIC**